Journal of Sound and Vibration (2001) **248**(3), 461–475
doi:10.1006/jsvi.2001.3793, available online at http://www.idealibrary.com on IDEAL®

A NOVEL TECHNIQUE IN BOUNDARY INTEGRAL EQUATIONS FOR ANALYZING ACOUSTIC RADIATION FROM AXISYMMETRIC BODIES

J. Zhao, G. R. Liu, H. Zheng, C. Cai and K. Y. Lam

Institute of High Performance Computing, 89-*C Science Park Drive*, *Singapore Science Park I*, 118261 *Singapore*. *E-mail*: *zhengh@ihpc.nus.edu.sg*

(*Received* 5 *July* 2000, *and in final form* 9 *March* 2001)

A novel technique is suggested to avoid singular integrals of boundary integral equations (BIE) for exterior sound radiation problems. The technique, reproduction of diagonal terms (RDT), utilizes special solutions of some monopole sources, which give the distribution of theoretical surface pressure and velocity to reproduce diagonal terms in the BIE matrices. It is proposed to employ three monopole sources in reproduction of diagonal terms in both pressure and velocity matrices. Although the interior points are applied to generate monopole solutions, the concept is basically different from that of general interior Helmholtz equations. So the present technique is different from those traditional methods to improve BIE method through added interior Helmholtz equations. Several examples are presented to demonstrate the effectiveness of the proposed technique for closed axisymmetric surfaces. Numerical results show that the technique of RDT can improve the accuracy of the solution up to 10 times compared to the conventional techniques such as SHF, CHIEF-SHF.

© 2001 Academic Press

1. INTRODUCTION

Research on boundary integral equations (BIE) for analyzing acoustic radiation from closed surface has being carried on since the 1960s. One of the key points of interest is how to solve the singular integral kernels and non-uniqueness of solution at certain characteristic frequencies concerned with internal Dirichlet problem.

The singularity problem occurs when the field point coincides with the point on the boundary during manipulation of boundary integral equations. A comprehensive survey of various methods for handling singularity and non-uniqueness problems of BIE was given by Benthien and Schenck [1]. Chertock used surface Helmholtz formulation (SHF) to analyze the acoustic radiation from an arbitrary body [2]. Copley suggested using internal Helmholtz equation to avoid singular integrals [3]. Copley's method, however, is effective for low-frequency range, because the interior points may coincide with interior nodes of standing wave at characteristic frequencies. When this occurs, the method results in invalid equations. Such a coincident probability is much higher at a higher frequency range. Schenck then developed a procedure called combined Helmholtz integral equation formulation (CHIEF) to improve the reliability [4]. The concept is to combine SHF and internal Helmholtz formulation at interior points, constructing over-determining matrix equations. Theoretically, CHIEF has not solved the non-uniqueness problem as the selected interior points may still coincide with internal standing wave nodes. Various efforts were

0022-460X/01/480461 + 15 $35.00/0 © 2001 Academic Press

made to improve CHIEF in the past. Piaszczyk and Klosner [5] proposed to put extra field points in the exterior region and an iterative technique must be used to solve both the surface pressure distribution and the pressures at the exterior points. Zhao *et al.* [6] further combined the internal equations with its associated first order derivatives to its reference co-ordinates to give more reliable internal equations for CHIEF method. Wu and Seybert suggested CHIEF blocks, a group of interior points, to use both internal Helmholtz formulation and their three first order derivatives as supplementary equations [7].

Off boundary collocation (OBC) method was proposed for removing the non-uniqueness problem in a manner similar to CHIEF [8]. Only interior Helmholtz formulation is used rather than surface Helmholtz formulation when using OBC method. The interior collocation points are taken to lie on a surface S' interior to actual surface S. OBC method avoids the singularity problem since the integration points and collocation points never coincide. Benthien and Schenck [1] pointed out that the solution to some cases is still not unique when the frequency equals a natural frequency of the interior Dirichlet problem for S'. Koopmann *et al.* [9] presented a method that uses the principle of wave superposition for computing the acoustic fields of arbitrarily shaped radiators. The wave superposition method has the advantage of avoiding the singularities in the Green function and also allows a cruder integration scheme. An array of monopole and dipole sources with unknown strength is placed on a surface S' interior to S. The pressure that satisfies the surface Helmholtz formulation is expressed as the superposition of sound radiated by the monopole and dipole sound sources. Hence, the source strengths of the sources can be calculated based on the velocity prescribed on the surface S. The strengths of the sources that produce this condition can, in turn, be used to compute the corresponding surface pressures. In most cases, wave superposition method tends to be much faster than CHIEF and OBC methods since there are no integrals involved.

Burton and Miller presented a method for the non-uniqueness problem by combining SHF with its normal derivatives [10]. However, its hyper-singular integrals are more difficult to be handled. Many researches [11–15] were dedicated to reduce the singularity order and improve the computing efficiency. The boundary point method was presented for analyzing the acoustic radiation problems caused by a vibrating surface [16]. The coefficient matrices in surface Helmholtz formulation are replaced by the particular solution matrices generated by a set of fabricated sources. These fabricated sources are constructed along the normal lines of the nodes on the surface S. The boundary point method can avoid the singular integration and overcome the non-uniqueness problem at the characteristic frequencies effectively.

The present paper is devoted to singular integral treatment in SHF. The technique proposed, reproduction of diagonal terms (RDT), can improve the integral accuracy in a manner similar to boundary point method. The difference between them is that, in RDT, only diagonal terms in the pressure/velocity matrices are calculated by using non-diagonal terms and a few interior monopole solutions. The procedure to fulfill the task is as follows:

(1) putting monopole point sources in interior points;
(2) calculating their theoretical pressures and velocities distributed on the surface;
(3) substituting known pressures and velocities of the monopole point sources to the matrix equation, whose diagonal terms are taken as variables and thus evaluated;
(4) computing non-diagonal terms of pressure and velocity matrix through direct integration procedure for SHF, without any singularity;
(5) applying the ultimate matrix equation for surface pressure calculations.

2. MATHEMATICAL FORMULATIONS

The general Helmholtz integral formulation for exterior acoustic field is described as [17]

$$C(\alpha)P(\alpha) = \int_S \int \left[P(\beta) \frac{\partial G(\alpha, \beta)}{\partial n_\beta} + \mathrm{j}k\rho c V(\beta) G(\alpha, \beta) \, \mathrm{d}S_\beta \right], \tag{1}$$

where α denotes a field point which may be within, on or outside of the surface. β denotes a point on the surface S. $C(\alpha)$ is 0 for an interior field point α; 4π for an exterior field point and 2π for smoothed surface field point α. For a surface field point α with discontinuous normal, $C(\alpha)$ is a solid angle in exterior media area and may be represented as

$$C(\alpha) = 4\pi + \int_S \int \frac{\partial}{\partial n_\beta} \left(\frac{1}{d(\alpha, \beta)} \right) \mathrm{d}S_\beta, \tag{2}$$

where $d(\alpha, \beta)$ is the distance between the field point α and point β on the surface S, P and V denote acoustic pressure and velocity on the surface S, respectively, ρ and c denote density and sound speed in the acoustic media, respectively, $G(\alpha, \beta) = \exp(-\mathrm{j}kd(\alpha, \beta)/d(\alpha, \beta)$, k represents wave number and $\mathrm{j}^2 = -1$.

Consider a closed axisymmetric surface, equations (1) and (2) can be further deduced to

$$\begin{aligned} C(\alpha)P(\alpha) = {} & \int_0^L P(\beta) \, \mathrm{d}l_\beta \int_0^{2\pi} \frac{1 + \mathrm{j}kd(\alpha, \beta)}{d^3(\alpha, \beta)} \mathrm{e}^{-\mathrm{j}kd(\alpha, \beta)} \\ & \left(\frac{\mathrm{d}r_\beta}{\mathrm{d}l_\beta} (x_\beta - x_\alpha) - \frac{\mathrm{d}x_\beta}{\mathrm{d}l_\beta} (r_\beta - r_\alpha \cos(\theta_\beta - \theta_\alpha)) \right) r_\beta \, \mathrm{d}\theta_\beta \\ & + \int_0^L \rho c V(\beta) \, \mathrm{d}l_\beta \int_0^{2\pi} \frac{\mathrm{e}^{-\mathrm{j}kd(\alpha, \beta)})}{d(\alpha, \beta)} \mathrm{j}kr_\beta \, \mathrm{d}\theta_\beta, \end{aligned} \tag{3}$$

$$C(\alpha) = 4\pi + \int_0^L \mathrm{d}l_\beta \int_0^{2\pi} \frac{1}{d^3(\alpha, \beta)} \left(\frac{\mathrm{d}r_\beta}{\mathrm{d}l_\beta} (x_\beta - x_\alpha) - \frac{\mathrm{d}x_\beta}{\mathrm{d}l_\beta} (r_\beta - r_\alpha \cos(\theta_\beta - \theta_\alpha)) \right) r_\beta \, \mathrm{d}\theta_\beta), \tag{4}$$

where L is the total length of the meridian curve, l is the meridian co-ordinate, θ is the angular co-ordinate along the circular direction, and r is the distance between the surface point and symmetric axis. As shown in Figure 1, l and r are determined by surface shapes. The distance between points α and β is

$$d(\alpha, \beta) = \sqrt{(x_\beta - x_\alpha)^2 + (r_\beta - r_\alpha)^2 + 4r_\beta r_\alpha \sin^2 \frac{\theta_\beta - \theta_\alpha}{2}}. \tag{5}$$

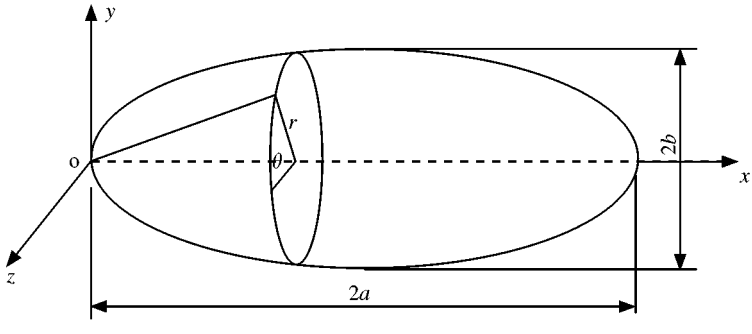

Figure 1. Illustration of a general axisymmetric surface.

Equation (3) shows that both integral terms in the right-hand side are singular when the field point α approaches the point β on the surface.

In a practical numerical model, a Gauss integration procedure with even numbers of Gauss sampling points may be used for a direct evaluation of the above singular integrals. Zhao *et al.* [18] used a formula based on polar co-ordinate transform to eliminate the singularity of axisymmetric surfaces; the calculating accuracy was raised significantly by about 10 times in comparison with that of direct Gauss integration. However, the introduced formulation is very complicated and requires the second order derivatives which are more difficult to be obtained for arbitrary surface shapes.

The new technique RDT proposed in this paper is based on the premise that theoretical solutions of surface pressure and velocity distribution can be obtained for a monopole point source. Suppose the monopole point source γ is placed within the internal space, then the sound pressure and particle velocity at a point α can be expressed as

$$P_\gamma(\alpha) = \frac{\exp(-\mathrm{j}kd(\gamma,\alpha))}{d(\gamma,\alpha)}, \tag{6}$$

$$V_\gamma(\alpha) = \frac{1+\mathrm{j}kd(\gamma,\alpha)}{\mathrm{j}kd(\gamma,\alpha)} \frac{\partial d(\gamma,\alpha)}{\partial n_\alpha} \frac{P_r(\alpha)}{\rho c}. \tag{7}$$

In general SHF, consider a hypothetical case with the field point α placed at node 1. The acoustic pressures and normal components of the vibration velocities of the surface at every node from 1 to n can be calculated using equation (3). This yields the first equation. To produce the second linear equation, the field point α is now placed at node 2 and equation (3) is used again to calculate all variables at other nodes. This operation is repeated until the field point α has covered all the n nodes. It will give n equations. These n equations will provide unique solutions to the n unknowns. To express these n equations in matrix form, we have

$$[A]\{P\} = [B]\{V\}, \tag{8}$$

where $[A]$ and $[B]$ are $n \times n$ matrices, related to surface pressure and velocity vectors respectively, n denotes the number of surface nodes. Linear interpolation is used for surface pressure and velocity distributions. $\{P\}$ and $\{V\}$ are $n \times 1$ column vectors.

Let

$$[F] = \begin{pmatrix} 0 & a_{12} & a_{13} & \cdots & \cdots & a_{1n} \\ a_{21} & 0 & a_{23} & \cdots & \cdots & a_{2n} \\ a_{31} & a_{32} & 0 & \cdots & \cdots & a_{3n} \\ \cdots & \cdots & \cdots & \cdots & \cdots & \cdots \\ \cdots & \cdots & \cdots & \cdots & \cdots & \cdots \\ a_{n1} & a_{n2} & a_{n3} & \cdots & \cdots & 0 \end{pmatrix}, \tag{9}$$

$$[H] = \begin{pmatrix} 0 & b_{12} & b_{13} & \cdots & \cdots & b_{1n} \\ b_{21} & 0 & b_{23} & \cdots & \cdots & b_{2n} \\ b_{31} & b_{32} & 0 & \cdots & \cdots & b_{3n} \\ \cdots & \cdots & \cdots & \cdots & \cdots & \cdots \\ \cdots & \cdots & \cdots & \cdots & \cdots & \cdots \\ b_{n1} & b_{n2} & b_{n3} & \cdots & \cdots & 0 \end{pmatrix}, \tag{10}$$

where a_{ij} and b_{ij} are the off-diagonal terms in matrices $[A]$ and $[B]$ respectively. Substituting $[F]$, $[H]$ in equations (9) and (10) into equation (8) yields

$$\begin{Bmatrix} P_\gamma(\alpha_1)\,a_{11} - V_\gamma(\alpha_1)\,b_{11} \\ P_\gamma(\alpha_2)\,a_{22} - V_\gamma(\alpha_2)\,b_{22} \\ P_\gamma(\alpha_3)\,a_{33} - V_\gamma(\alpha_3)\,b_{33} \\ \cdots \\ \cdots \\ P_\gamma(\alpha_n)\,a_{nn} - V_\gamma(\alpha_n)\,b_{nn} \end{Bmatrix} = -F\{P_\gamma\} + H\{V_\gamma\}, \tag{11}$$

where α_i is the field point on the surface.

As $P_\gamma(\alpha_i)$ does not equal 0, both sides of equation (11) can be divided by $P_\gamma(\alpha_i)$. Let $C_\gamma(\alpha_i) = V_\gamma(\alpha_i)/P_\gamma(\alpha_i)$, $\{D_\gamma(\alpha)\} = \{-[F]\{P_\gamma\} + [H]\{V_\gamma\}\}./\{P_\gamma(\alpha)\}$, where ./ indicates that each row term of the left vector is divided by the same row term of the right vector. Therefore,

$$a_{ii} - C_\gamma(\alpha_i)\,b_{ii} = D_\gamma(\alpha_i), \tag{12}$$

$$C_\gamma(\alpha_i) = \frac{1}{\rho c}\left(1 + \frac{1}{\mathrm{j}kd(\gamma, \alpha_i)}\right)\exp(-\mathrm{j}kd(\gamma, \alpha_i))\frac{\partial d(\gamma, \alpha_i)}{\partial n_{\alpha_i}}. \tag{13}$$

It is seen that all diagonal terms a_{ii}, b_{ii} $(i = 1, 2, 3, \ldots, n)$ can be obtained from equation (12) by choosing several monopole point sources located at γ_i $(i = 1, 2, 3, \ldots)$. From equation (13), $C_{\gamma_1}(\alpha_i) = C_{\gamma_2}(\alpha_i)$ occurs only if both $d(\gamma_1, \alpha_i) = d(\gamma_2, \alpha_i)$ and $\partial d(\gamma_1, \alpha_i)/\partial n_{\alpha_i} = \partial d(\gamma_2, \alpha_i)/\partial n_{\alpha_i}$ (if they are not equal to 0) are satisfied. Two internal monopole sources may not be enough as $C_{\gamma 1}(\alpha_i) = C_{\gamma 2}(\alpha_i)$ may occur, which results in non-existential values for a_{ii} and b_{ii}. For different kinds of surfaces, the following three schemes are suggested to ensure existential solutions.

(1) For an axisymmetric surface, three points that are on a line may be chosen. The requirement is that no surface point should be on the same line with perpendicular normal to it. Definitely, in this case, $d(\gamma_1, \alpha_i) = d(\gamma_2, \alpha_i) = d(\gamma_3, \alpha_i)$ are never satisfied for any α_i on the surface with finite distance from source points. However, if there exists a point α_i on the same and its normal direction is perpendicular to this line, that means $\partial d(\gamma_1, \alpha_i)/\partial n_{\alpha 1} = \partial d(\gamma_2, \alpha_i)/\partial n_{\alpha i} = \partial d(\gamma_3, \alpha_i)/\partial n_{\alpha i} = 0$, i.e., $C_{\gamma 1}(\alpha_i) = C_{\gamma 2}(\alpha_i) = C_{\gamma 3}(\alpha_i) = 0$, such a combination will not be effective.

(2) For general two-dimensional problems, three points may also be chosen. These points are on a circle within the closed surface and are not on the same line. In this case, $d(\gamma_1, \alpha_i) = d(\gamma_2, \alpha_i) = d(\gamma_3, \alpha_i)$ are never satisfied, and $C_{\gamma 1}(\alpha_i) = C_{\gamma 2}(\alpha_i) = C_{\gamma 3}(\alpha_i) = 0$ will never occur.

(3) For general three-dimensional problems, four points may be chosen, which are on a spherical surface within the closed surface and are not in the same plane. In this case, $d(\gamma_1, \alpha_i) = d(\gamma_2, \alpha_i) = d(\gamma_3, \alpha_i) = d(\gamma_4, \alpha_i)$ are never satisfied, and $C_{\gamma 1}(\alpha_i) = C_{\gamma 2}(\alpha_i) = C_{\gamma 3}(\alpha_i) = C_{\gamma 4}(\alpha_i) = 0$ will never occur.

In practice, for each α_i, the maximum absolute values of $abs(C_{\gamma 1}(\alpha_i) - C_{\gamma 2}(\alpha_i))$, $abs(C_{\gamma 1}(\alpha_i) - C_{\gamma 3}(\alpha_i))$, and $abs(C_{\gamma 2}(\alpha_i) - C_{\gamma 3}(\alpha_i))$ are compared. Two points with maximum coefficient difference are then used to calculate a_{ii}, b_{ii}. For example, at α_i, if γ_1, γ_3 give the maximum value of difference, then from equation (12), the following equations are obtained:

$$b_{ii} = -\frac{D_{\gamma 1}(\alpha_i) - D_{\gamma 3}(\alpha_i)}{C_{\gamma 1}(\alpha_i) - C_{\gamma 3}(\alpha_i)}, \tag{14}$$

$$a_{ii} = C_{\gamma 1}(\alpha_i)\,b_{ii} + D_{\gamma 1}(\alpha_i). \tag{15}$$

One more advantage of the RDT technique is that the diagonal term of a corner node is automatically determined by a general RDT procedure without the need to calculate the solid angle by equation (2) or (4).

To ensure the effectiveness and efficiency in handling singular integrals, the distance between vicinity nodes should be adequately smaller than the correspondent wavelength.

The CHIEF method relies on the validity of the supplement internal Helmholtz equation. At higher frequency, it is uncertain to determine whether the selected point is sufficiently apart from the nodes of the standing wave field. Considering that the distance between those standing wave nodes is of its wavelength scale, a practical scheme is suggested in this paper to fix only one point on the axis, and the others are apart from this reference point with lengths in fractions of half-wavelength, say 1/4, 2/4, 3/4, … . If one point coincides with the standing wave node, those other points may be close to the peak. For general three-dimensional acoustic radiation problem, as one point is fixed, those relative interior points may be selected on spherical surfaces (in different directions) with radius of 1/4, 2/4, 3/4 half-wavelength. In this way, the CHIEF method is improved in a wider frequency range. After interior Helmholtz equations are obtained, a procedure of least-squares method is employed to solve the over-determined matrix equations.

3. NUMERICAL EXAMPLES

3.1. SPHERICAL SURFACE

Let n be the node number along a spherical meridian line. In the following calculation examples, four point Gauss integration procedure is employed. In the circular direction, it is divided into $n_c - 1$ segments. For a spherical surface,

$$n_c = 2(n-1)\frac{r}{R_0} + 1, \tag{16}$$

where R_0 is the radius of the spherical surface; r is the radius of a profile circle or the distance from the surface point to the symmetric axis.

For axisymmetric surfaces, four interior points for CHIEF are placed on the symmetric axis. The fixed point coincides with the spherical centre ($x = R_0$), other points are put at $x = R_0 + 0{\cdot}5\lambda \times 1/4$, $R_0 + 0{\cdot}5\lambda \times 2/4$, $R_0 + 0{\cdot}5\lambda \times 3/4$ ($0{\cdot}5\lambda$ is half-wavelength) from this reference point.

The characteristic frequency for the spherical surface is $kR_0 = \pi, 2\pi, 3\,\pi, 4\pi, 5\pi, \ldots$; and the interior point sources (PS_1, PS_2, PS_3) for RDT are placed on axis at $x = 0{\cdot}9R_0$, $1{\cdot}1R_0$, $1{\cdot}3R_0$.

In Figures 2–4, $n = 17$, the velocity distribution is given by the interior point source at spherical centre ($x = R_0$). The relative error is obtained through the difference between the calculated pressure distribution and the theoretical solution.

Figure 2 compares the relative error of the calculated surface pressure with respect to its theoretical one when a point source is placed at the spherical centre. It shows that the relative errors increase as the frequency increases, and the relative error of SHF method becomes extraodinarily high around the characteristic frequencies. CHIEF method, either combined with SHF, called CHIEF-SHF or with RDT, called CHIEF-RDT, provides a unique solution in the frequency range interested. The introduction of RDT has two effects on the calculations. First, it actually improves the accuracy up to 10 times (compare the curves of SHF/RDT, or CHIEF-SHF/CHIEF-RDT). Second, without using CHIEF, RDT surprisingly provides an improved solution at those characteristic frequencies! The

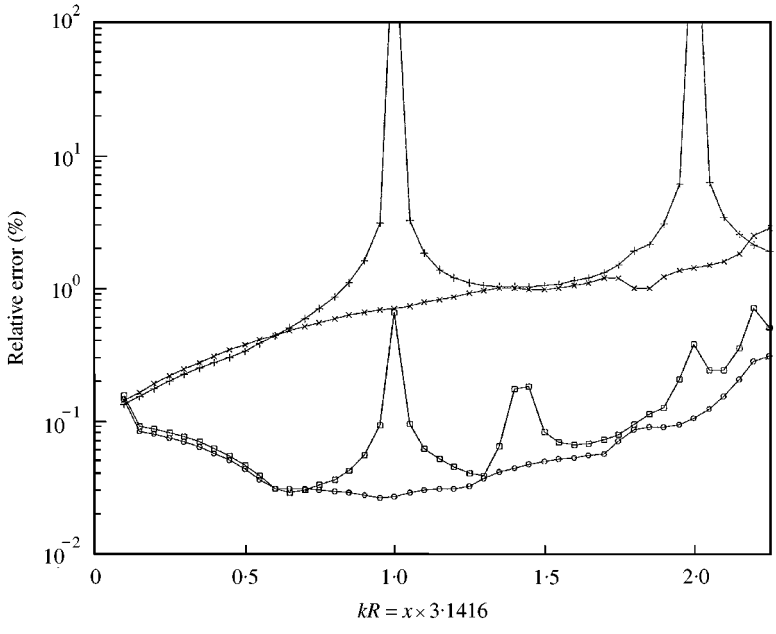

Figure 2. The maximum relative error (%) of the theoretical and calculated surface pressure by various methods for a spherical surface: —+—, SHF; —□—, RDT; —×—, CHIEF-SHF; —○—, CHIEF-RDT.

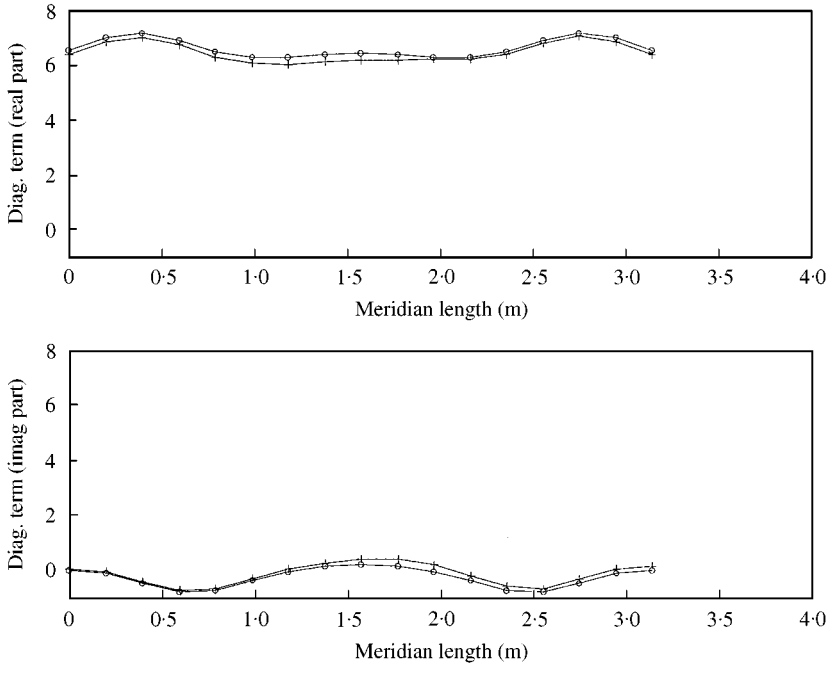

Figure 3. Diagonal terms of pressure matrix for a spherical surface calculated by SHF and RDT, $kR_0 = \pi$: —○—, SHF; —+—, RDT.

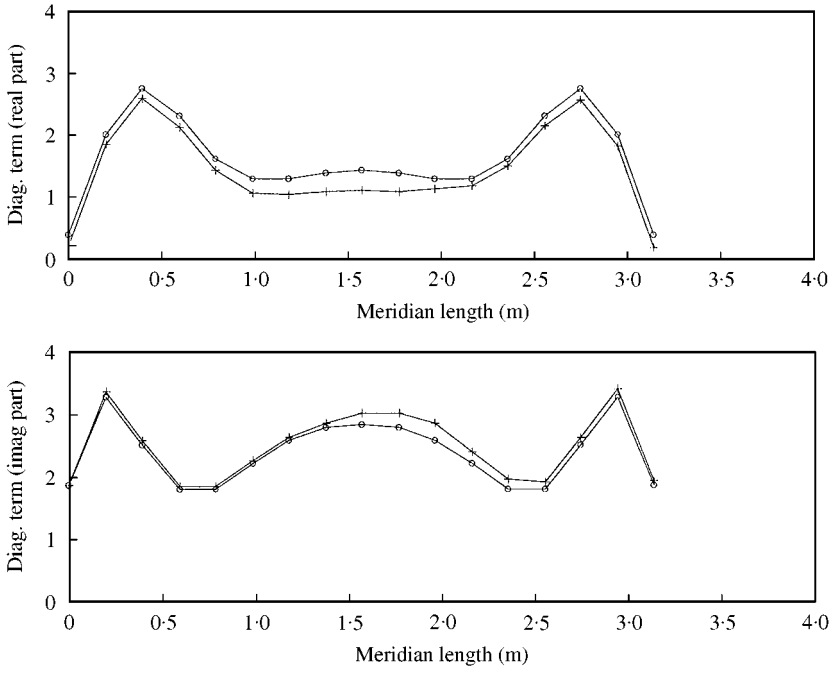

Figure 4. Diagonal terms of velocity matrix for a spherical surface calculated by SHF and RDT, $kR_0 = \pi$: -o-, -+-, SHF; —|—, RDT.

reason for this may be that those interior monopole sources used to calculate diagonal terms change the properties of the matrix equation, leading to the result that the RDT method is less sensitive to non-uniqueness problem.

Figures 3 and 4 show diagonal terms computed by SHF and RDT. There are some differences between two kinds of curves, which may partly be related to the introduction of point sources. As the interior points are not placed symmetrically, those diagonal terms are also not symmetric. For a symmetric velocity distribution of velocity, the calculated pressure distribution remains symmetric, which is not affected by the non-symmetrical arrangement of interior point sources.

The results of relative errors at six characteristic frequencies are listed in Table 1. SHF is definitely invalid. RDT gives correct results and its accuracy is better than that of CHIEF-SHF. CHIEF-RDT gives the best results among these four methods.

TABLE 1

Comparison of the maximum relative error (%) *of theoretical and calculated surface pressures at characteristic frequencies for a spherical surface* (*node number*: 41)

	$kR_0 = \pi$	$kR_0 = 2\pi$	$kR_0 = 3\pi$	$kR_0 = 4\pi$	$kR_0 = 5\pi$	$kR_0 = 6\pi$
SHF	636%	1260%	1884%	2508%	3129%	3746%
RDT	0·66%	0·28%	0·29%	0·19%	0·19%	0·22%
CHIEF-SHF	0·34%	0·73%	1·51%	0·96%	1·60%	1·76%
CHIEF-RDT	0·00%	0·02%	0·10%	0·05%	0·06%	0·12%

3.2. SPHEROID SURFACE

Consider further a spheroid axisymmetric surface with $n = 17$ and $b/a = 0{\cdot}5$ are shown in Figure 1.

For spheroid surfaces, four interior points for CHIEF are placed on the symmetric axis. The fixed point coincides with the spherical centre ($x = a$), other points are placed at $x = a + 0{\cdot}5\lambda \times 1/4$, $R_0 + 0{\cdot}5\lambda \times 2/4$, $R_0 + 0{\cdot}5\lambda \times 3/4$ ($0{\cdot}5\lambda$ is half-wavelength) from this reference point. The point sources (PS_1, PS_2, PS_3) for RDT are placed on axis at $x = 0{\cdot}9a$, $1{\cdot}1a$, $1{\cdot}3a$.

In Figures 5–7, the results are based on the velocity distribution of an internal point source at the spheroid centre ($x = a$). The relative error is obtained through the difference between the calculated pressure distribution and the theoretical solution. Figure 5 shows the relative errors of the calculated surface pressures with its theoretical ones when a point source is placed at the spheroid centre. The characteristic frequency is about $ka = 5{\cdot}34$. Figures 6 and 7 show the diagonal terms computed by SHF and RDT. The results of the spheroid surface are consistent with that of the spheroid surface.

3.3. FINITE CYLINDRICAL SURFACE

The geometry of a finite cylinder is shown in Figure 8. The surface is also divided into $n - 1$ segments along the meridian direction. The cylindrical surface and two end plates are intersected, which results in two corner nodes. According to equation (4), the solid angles on these corner nodes are 3π, rather than 2π for smoothed surface nodes. In using RDT to avoid singular integrals, each corner edge should be represented by two nodes, one is on the end plate and the other one is on the cylindrical surface, thus their surface normal is unique for using the interior point source solution.

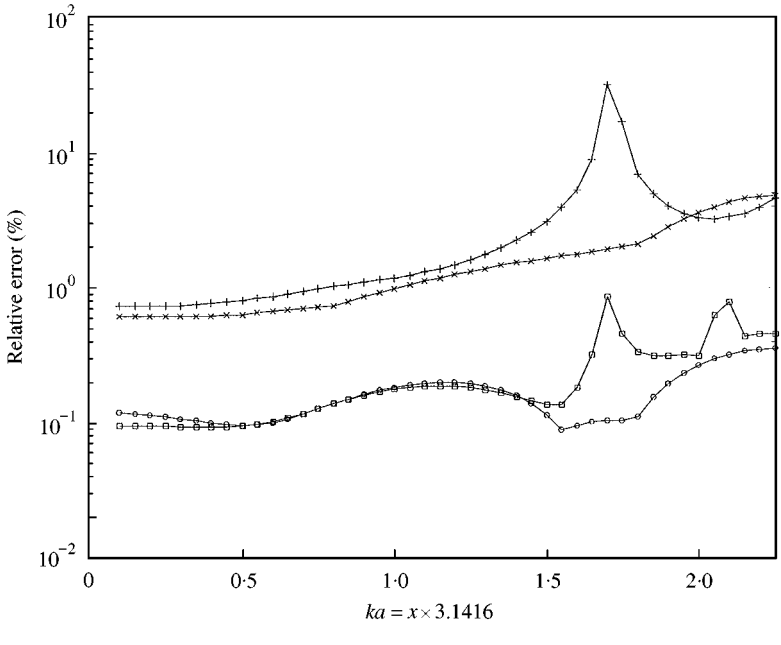

Figure 5. The maximum relative error (%) of theoretical and calculated surface pressure by various methods for a spheroid surface, $b/a = 0{\cdot}5$: ⊣+⊢, SHF; ⊣□⊢, RDT; ⊣×⊢, CHIEF-SHF; ⊣○⊢, CHIEF-RDT.

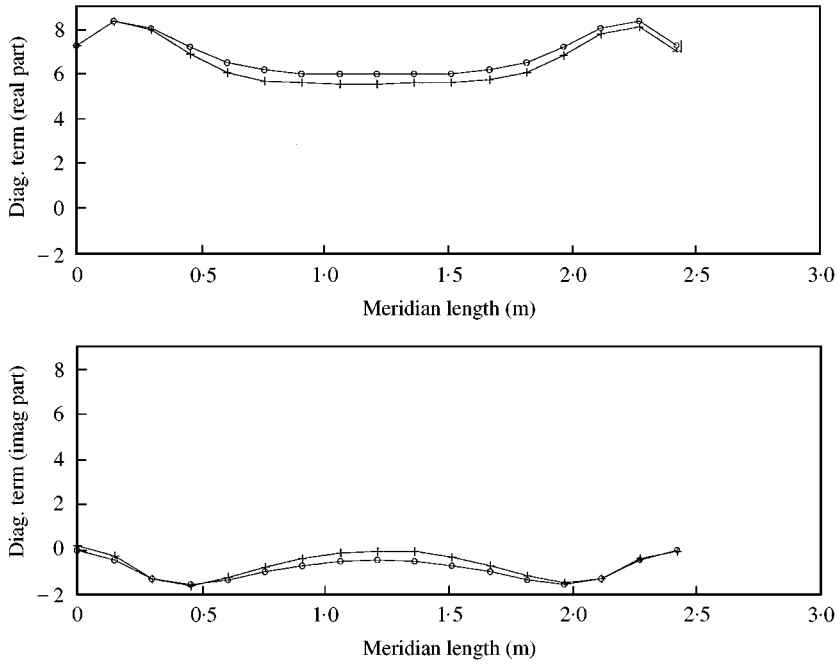

Figure 6. Diagonal terms of pressure matrix for a spheroid surface calculated by SHF and RDT, $ka = 5{\cdot}34$, $b/a = 0{\cdot}5$: ⊸, SHF; ⊣, RDT.

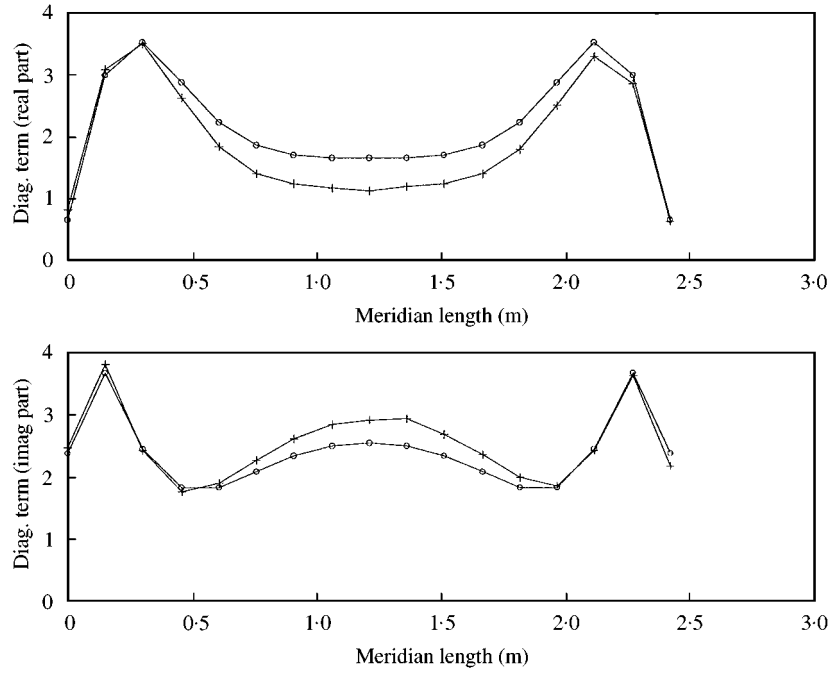

Figure 7. Diagonal terms of velocity matrix for a spherical surface calculated by SHF and RDT, $ka = 5{\cdot}34$, $b/a = 0{\cdot}5$: ⊸, SHF; ⊣, RDT.

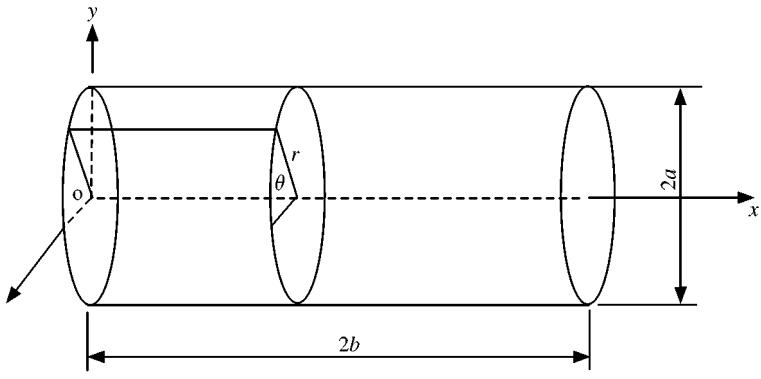

Figure 8. Illustration of a finite cylinder.

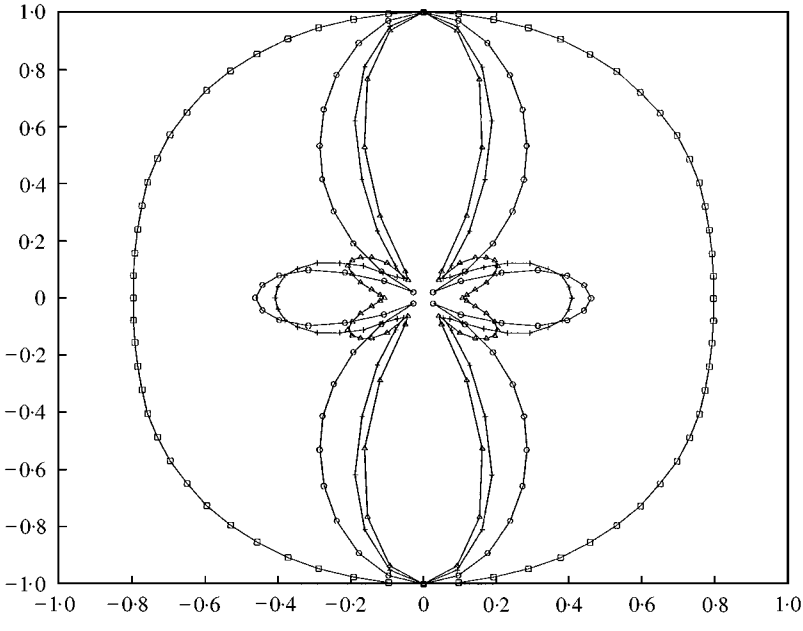

Figure 9. Directional pattern of farfield pressure from finite cylinder (CHIEF-RDT), $ka = 1, 2, 2{\cdot}53, 3$, $b/a = 2$: ⊟, $ka = 1$; ○, $ka = 2$; +, $ka = 2{\cdot}53$; △, $ka = 3$.

In this example, $b/a = 2$, $n = 33$. Seven nodes are placed on each end plate, and 19 nodes are placed on the cylindrical surface. In the circular direction, it is divided into n_c-1 segments.

$$n_c = \frac{2\pi r}{\Delta l} + 1, \tag{17}$$

where Δl is the average segment length along the meridian line; r is the radius of the profile circle, or the distance from surface point to the symmetric axis. A point source is placed in the geometric centre ($x = b$).

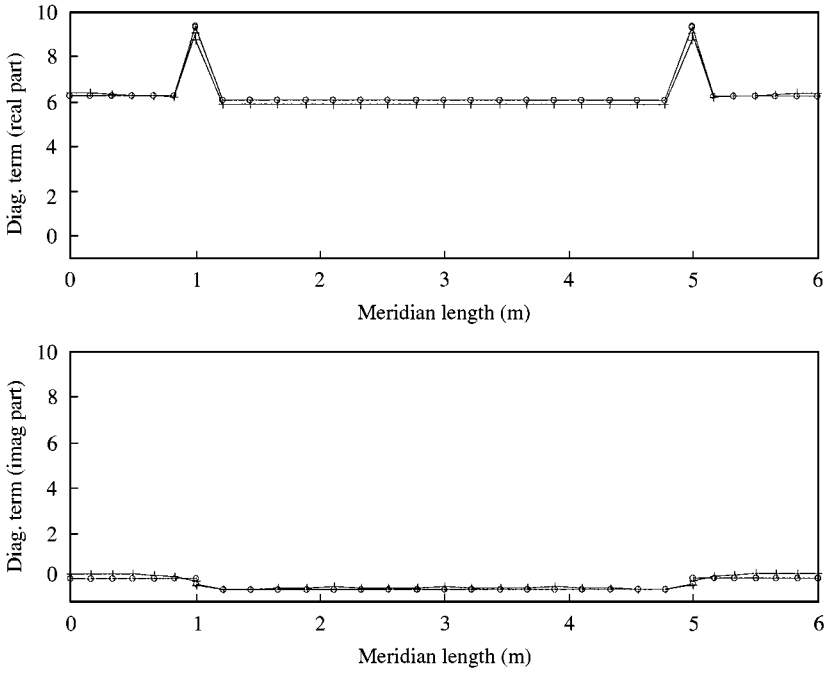

Figure 10. Diagonal terms of pressure matrix for a finite cylinder calculated by SHF and RDT, $ka = 2{\cdot}53$, $b/a = 2$: ⊸, SHF; ⊣, RDT.

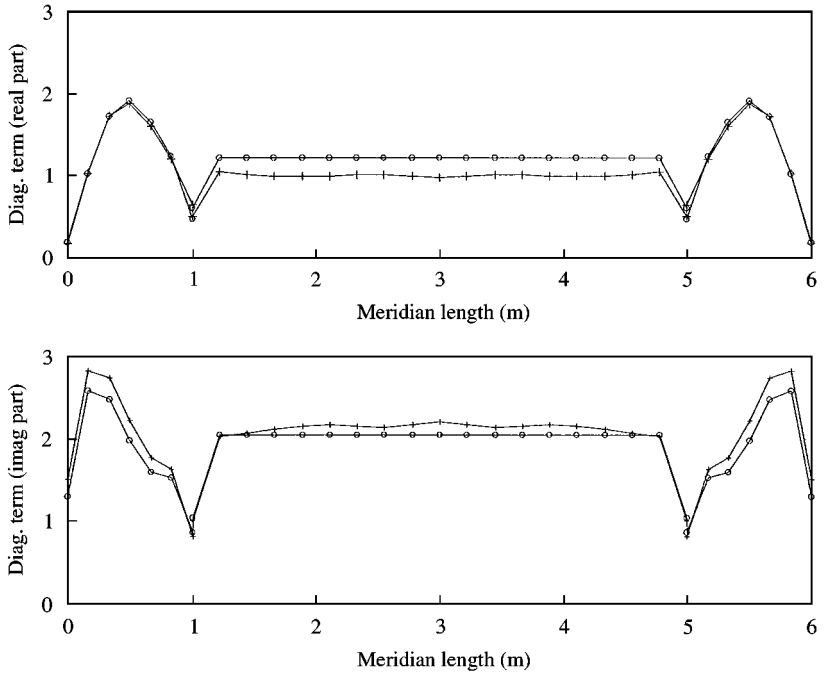

Figure 11. Diagonal terms of velocity matrix for a finite cylinder calculated by SHF and RDT, $ka = 2{\cdot}53$, $b/a = 2$: ⊸, SHF; ⊣, RDT.

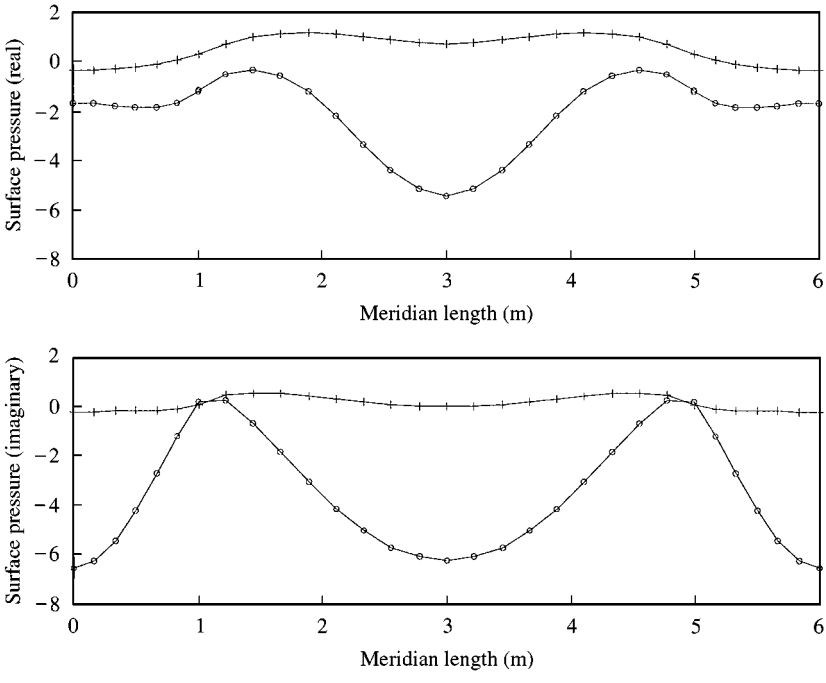

Figure 12. Surface pressure distribution for a finite cylinder calculated by SHF and RDT, $ka = 2{\cdot}53$, $b/a = 2$: —o—, SHF; —+—, RDT.

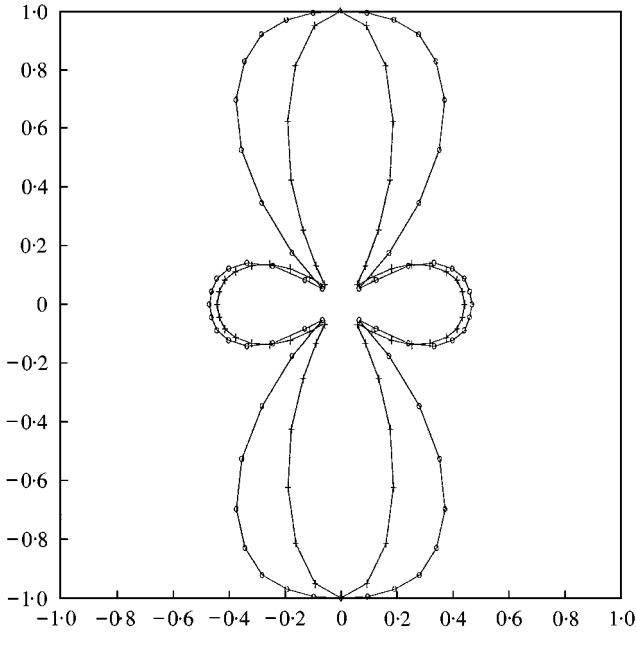

Figure 13. Directional pattern of farfield pressure from finite cylinder calculated by SHF and RDT, $ka = 2{\cdot}53$, $b/a = 2$: —o—, SHF, —+—, RDT.

For CHIEF interior point selection, the fixed point is the same as the geometric centre ($x = b$), the other three points are relatively $x = b + 0{\cdot}5\lambda \times 1/4$, $b + 0{\cdot}5\lambda \times 2/4$, and $b + 0{\cdot}5\lambda \times 3/4$ ($0{\cdot}5\lambda$ is half-wavelength) apart from this fixed point along the axial direction. For RDT, the interior three monopole sources are placed on symmetric axis: $x = 0{\cdot}5b$, b, and $1{\cdot}5b$ respectively. The surface normal velocity distribution is uniform on the cylindrical surface, and is zero on two end plates.

Figure 9 shows the farfield pattern at $ka = 1$, 2, 2·53, and 3 by CHIEF-RDT, which are very close to those reported in references [4, 6]. Figures 10 and 11 show the diagonal terms calculated by SHF or RDT. In Figures 12 and 13, the comparisons of surface pressure distributions and farfield directional patterns of SHF and RDT at characteristic frequency ($ka = 2{\cdot}53$) are shown. It can be seen from Figure 12 that the surface pressure (real and imaginary part) has no jumps at corner nodes (meridian length = 1 m, or 5 m).

4. CONCLUSION

In this paper, a novel technique, reproduction of diagonal terms (RDT), is proposed to avoid singular integrals in boundary integral equations (BIE) for acoustic radiation from axisymmetric surfaces.

To avoid singular integrals in surface Helmholtz formulation (SHF), RDT uses three monopole point sources placed in the interior space for an axisymmetric acoustic problem. The given theoretical distributions of surface pressure and velocity of three monopole point sources, respectively, are then applied to determine the diagonal terms of pressure/velocity matrices. When a corner node is encountered, its diagonal terms are automatically estimated, without the need to calculate a solid angle. The numerical examples for spherical and spheroid surfaces show that the accuracy can be raised up to 10 times, especially effective at a higher frequency range.

The key issue to ensure the effectiveness of the above improvement of singularity handling is that the method requires the surface element to be divided sufficiently small. The technique developed in this article can be further applied for general two- or three-dimensional acoustic BEM.

REFERENCES

1. W. BENTHIEN and A. SCHENCK 1997 *Computers & Structures* **65**, 295–305. Nonexistence and nonuniqueness problems associated with integral equation methods in acoustics.
2. G. CHERTOCK 1964 *Journal of the Acoustical Society of America* **35**, 1305–1313. Sound radiation from an arbitrary body.
3. L. G. COPLEY 1966 *Journal of the Acoustical Society of America* **41**, 807–816. Integral equation method for radiating from vibrating bodies.
4. H. A. SCHENCK 1968 *Journal of the Acoustical Society of America* **44**, 41–58. Improved integral formulation for acoustic radiation problems.
5. C. M. PIASZCZYK and J. M. KLOSNER 1984 *Journal of the Acoustical Society of America* **75**, 363–375. Acoustic radiation from vibrating surfaces at characteristic frequencies.
6. J. ZHAO, H. Z. WANG and W. H. ZHU 1989 *Chinese Journal of Acoustics* **8**, 111–120. Boundary element method for calculating acoustic radiation from closed surface with prescribed velocity distribution.
7. T. W. WU and A. F. SEYBERT 1991 *Journal of the Acoustical Society of America* **90**, 1608–1614. A weighted residual formulation for the CHIEF method.
8. J. D. ACHENBACH, J. D. KECHTER and Y. L. XU 1988 *Computer Methods in Applied Mechanics and Engineering* **70**, 191–201. Off boundary approach to the boundary element method.

9. G. H. KOOPMANN, L. SONG and J. B. FAHNLINE 1989 *Journal of the Acoustical Society of America* **86**, 2433–2438. A method for computing acoustic fields based on the principle of wave superposition.
10. A. J. BURTON and G. F. MILLER 1971 *Proceedings of the Royal Society of London A* **323**, 201–210. The application of integral equation methods to the numerical solution of some exterior boundary value problems.
11. W. L. MEYER, W. A. BELL, M. P. STALLYBRASS and B. T. ZINN 1979 *Journal of the Acoustical Society of America* **65**, 631–638. Prediction of the sound field from axi-symmetric surfaces.
12. C. C. CHIEN, H. RAJIYAH and S. N. ATLURI 1990 *Journal of the Acoustical Society of America* **88**, 918–937. An effective method for solving the hypersingular integral equations in 3-D acoustics.
13. T. W. WU, A. F. SEYBERT and G. C. WAN 1991 *Journal of the Acoustical Society of America* **90**, 554–560. On the numerical implementation of a Cauchy principal value integral to insure a unique solution for acoustic radiation and scattering.
14. W. S. HWANG 1997 *Journal of the Acoustical Society of America* **101**, 3330–3335. A boundary integral method for acoustic radiation and scattering.
15. W. S. HWANG 1997 *Journal of the Acoustical Society of America* **101**, 3336–3342. Hypersingular boundary integral equations for exterior acoustic problems.
16. S. Y. ZHANG and X. Z. CHEN 1999 *Journal of Sound and Vibration*, **228**, 761–772. The boundary point method for the calculation of exterior acoustic radiation problem.
17. A. F. SEYBERT, B. SOENARKO, F. J. RIZZO and D. J. SHIPPY 1986 *Journal of the Acoustical Society of America* **80**, 1241–1247. A special integral equation formulation for acoustic radiation and scattering for axi-symmetric bodies and boundary conditions.
18. J. ZHAO, H. Z. WANG and W. H. ZHU 1989 *Journal of Shanghai Jiao Tong University* **23**, 61–69. An improved method for calculating sound radiation from axi-symmetric shells with boundary integral equation.